

Micromechanical Properties of Elastic Polymeric Materials As Probed by Scanning Force Microscopy

S. A. Chizhik,[†] Z. Huang,[‡] V. V. Gorbunov,[†] N. K. Myshkin,[†] and V. V. Tsukruk^{*,‡}

Metal-Polymer Institute, National Academy of Science, Gomel 246550, Belarus, and College of Engineering and Applied Sciences, Western Michigan University, Kalamazoo, Michigan 49008-5062

Received January 5, 1998

Scanning force microscopy (SFM) was used for probing micromechanical properties of compliant polymeric materials. Classic models of elastic contacts, Sneddon's, Hertzian, and JKR, were tested for various indentation depths and for a variety of polymeric materials. We selected extremely compliant polyisoprene rubbers (Young's modulus, $E = 1\text{--}3$ MPa), elastic polyurethanes ($E = 5\text{--}50$ MPa), and hard surfaces of polystyrene (PS) and polyvinylchloride (PVC) ($E = 1\text{--}5$ GPa). Both Sneddon's and Hertzian elastic models gave consistent and reliable results in the range of indentation depths up to 200 nm which are close to JKR solution. *Close correlation* is observed between absolute values of elastic moduli determined by SFM and known values for bulk materials.

Introduction

Local probing of surface mechanical properties with a submicron resolution became a reality after the introduction of atomic force microscopy (AFM) and subsequent development of the scanning force microscopy (SFM) technique.¹ The SFM ability to probe local surface topography, elastic surface properties, adhesive forces, and shear stresses on a submicron scale makes SFM unique for detecting micromechanical surface properties.^{2–13} However, the quantitative characterization of the micromechanical properties is still a challenge for SFM.⁹ Quantitative measurements require the knowledge of tip shape and cantilever spring constants.^{3,14} Optimal scanning conditions for the retrieval of reliable micromechanical data are needed to be defined.⁵ The types

of micromechanical contact should be clarified, and appropriate models of elastic contact should be chosen. This is especially true for very compliant polymeric materials with large elastic deformations, high adhesive forces, and viscoelastic behavior. These and other problems complicate SFM application to micromechanical studies of polymer surfaces.

In the present communication, we report the initial results from model studies on micromechanical properties of polymeric materials based on classic theories of elastic contacts, Sneddon's, Hertzian, and Johnson–Kendall–Roberts (JKR). These models were tested for a set of polymeric materials with Young's modulus E from 1 MPa to 5 GPa and indentation depths up to 200 nm.

Experimental Section

The samples for investigation were selected to represent a variety of polymeric materials with a wide range of elastic properties. Polyisoprene rubber, $M_w = 800\,000$ (Aldrich), had a nominal Young's modulus of 1–3 MPa.¹⁵ Polyester-based Elastollan polyurethanes (PUs) (BASF) and Dyreflex PU (Bayer) had Young's moduli in the range 10–40 MPa. Polyvinylchloride (PVC) was Selectophore from Fluka with a Young's modulus in the range 1–4 GPa. Polystyrene (PS) with $M_w = 250\,000$ and $E = 2\text{--}5$ GPa was obtained from Janssen Chimica. Smooth polymer films of several micrometer thickness were prepared by the spin-coating technique.

A combination of a contact mode in air and fluid and tapping and phase modes in air was used to characterize the polymers' surfaces according to the well-established procedure.^{4,16} The microscope used was the Dimension 3000 (Digital Instruments, Inc.). To evaluate the micromechanical properties, we analyzed 10–20 force–distance curves measured at three to six randomly selected locations, using an approach–retract frequency in the range from 0.02 to 183 Hz. The elimination of the capillary forces was achieved by scanning in fluid (MilliQ water and/or absolute alcohol).

We used a set of silicon and silicon nitride V-shaped cantilevers with spring constants k_n of 0.25, 0.5, 0.58, 0.7, and 21 N/m; stiffer cantilevers were applied to harder materials. Spring constants were determined and cross-checked by the fundamental resonant frequency calibration proposed earlier,¹⁷ the cantilever-against-

* To whom correspondence should be addressed. Fax: 616-387-6517. E-mail: vladimir@wmich.edu.

[†] National Academy of Science.

[‡] Western Michigan University.

(1) Binnig, G.; Quate, C. F.; Gerber, Ch. *Phys. Rev. Lett.* **1986**, *12*, 930. Sarid, D. *Scanning Force Microscopy*; Oxford University Press: New York, 1991.

(2) *Scanning Probe Microscopy of Polymers*; Ratner, B., Tsukruk, V. V., Eds.; ACS Symposium Series; American Chemical Society: Washington, DC, 1998; vol. 694.

(3) Overney, R.; Tsukruk, V. V. In *Scanning Probe Microscopy of Polymers*; Ratner, B., Tsukruk, V. V., Eds.; ACS Symposium Series; American Chemical Society: Washington, DC, 1998, vol. 694, p. 2.

(4) Tsukruk, V. V. *Rubber Chem. Technol.* **1997**, *70* (3), 430.

(5) Vanlandingham, M. R.; McKnight, S. H.; Palmese, G. R.; Ellings, J. R.; Huang, X.; Bogetti, T. A.; Eduljee, R. F.; Gillespie, J. W. *J. Adhesion* **1997**, *64*, 31.

(6) Vanlandingham, M. R.; McKnight, S. H.; Palmese, G. R.; Eduljee, R. F.; Gillespie, J. W.; McCulough, R. J. *J. Mater. Sci. Lett.* **1997**, *16*, 117.

(7) Wahl, K. L.; Stepnowski, S. V.; Unertl, W. L. *Tribol. Lett.*, accepted.

(8) Rosa-Zeiser, A.; Weilandt, E.; Hild, S.; Marti, O. *Meas. Sci. Technol.* **1997**, *8*, 1333.

(9) *Micro/Nanotribology and Its Applications*; Bhushan, B., Ed.; NATO ASI Series; Kluwer Academic Publishers: Dordrecht, 1997.

(10) Burnham, N. A.; Colton, R. J. *J. Vac. Sci. Technol.* **1989**, *A7*, 2906.

(11) Hues, S. M.; Draper, C. F.; Colton, R. J. *J. Vac. Sci. Technol.* **1994**, *B12*, 2211.

(12) Tsukruk, V. V.; Everson, M.; Lander, L.; Brittain, W. *Langmuir* **1996**, *12*, 3905.

(13) Phart, G. M.; Oliver, W. C.; Brotzen, F. B. *J. Mater. Res.* **1992**, *7*, 613.

(14) Hues, S. M.; Colton, R. J.; Meyer, E.; Guntherodt, H.-J. *MRS Bull.* **1993**, *18* (1), 41.

(15) Aklonis, J. J.; MacKnight, W. J. *Introduction to Polymer Viscoelasticity*; J. Wiley & Sons: New York, 1983.

(16) Tsukruk, V. V.; Reneker, D. H. *Polymer* **1995**, *36*, 1791.

(17) Hazel, J.; Tsukruk, V. V. *J. Tribol.*, accepted.

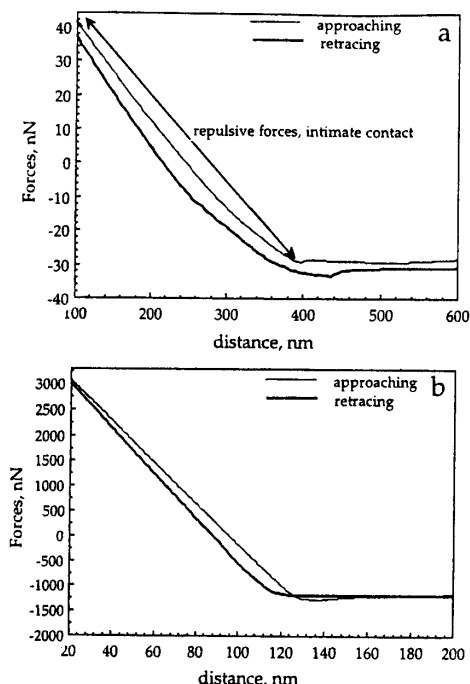


Figure 1. Force–distance data for the studied polymers in an approaching–retracing cycle. The force scale is in nanonewtons with an arbitrary zero level; distance is in nanometers with an arbitrary zero point. A thin line is the approaching cycle, and a bold line is the retracing cycle for all systems: (a) polyisoprene rubber, contact range used for analysis is shown by arrows; (b) PS.

cantilever technique, and the added mass technique (see review of different approaches in ref 17). Elastic response was controlled by the observation of indentation area after force measurements, and normal loads were selected to ensure an absence of indentation marks. To estimate tip end radius, we used a specially prepared sample of mixed gold nanoparticles tethered to a thiol-terminated SAM in accordance with the established procedure.¹⁸ Tip radii varied in the range 20–60 nm, from tip to tip.

Results and Discussion

Surface morphologies of all samples studied here were observed using tapping mode in air. Spin-coated films of 0.5–3- μm thickness possessed microroughness (calculated within 1 $\mu\text{m} \times 1 \mu\text{m}$ area) in the range 0.2–0.8 nm for PVC, PS, and rubber and 3–4 nm for PUs, respectively. Thus, all surfaces studied were smooth with random variation of elevations much smaller than the indentation depths explored in this work.

To verify the applicability of different theories of elastic contact, we used three different approaches, namely, Sneddon's, Hertzian, and JKR models.^{9,19,20} Initially, we analyzed the repulsive force in the approaching mode for the rubber sample (Figure 1a). All force–distance curves obtained show a sharp contact point, a repulsive range in the approaching part, and a pull-off point in the retracing

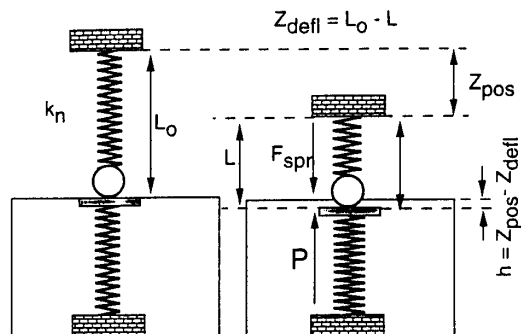


Figure 2. Double-spring model of elastic contact and major designations used in this work.

cycle. In this work, we limit ourselves to the analysis of the approaching part of the force–distance curves during intimate repulsive contact (see the designations in Figure 1a).

The equations for calculation of Young's modulus from cantilever deflection data can be derived by using a two-spring linear model of interacting cantilever spring and elastic surface (Figure 2). Conditions for quasi-static equilibrium for this model are presented as equality of cantilever spring forces exerted and elastic surface response:

$$k_n z_{\text{defl}} = P(h) \quad (1)$$

where $P(h)$ is normal load as a function of variable indentation depth $h = z_{\text{pos}} - z_{\text{defl}}$, z_{defl} is a measured vertical deflection of the SFM cantilever, and z_{pos} is the vertical displacement of the SFM piezoelement (Figure 2). By using known relationships between normal load $P(h)$ and materials and indentation parameters offered in elastic contact models, one can obtain analytical expressions of Young's modulus for each model.^{19,20} For the polymer systems considered here, we assume $E_{\text{tip}} \gg E_{\text{polymer}}$ and, therefore, $E = E_{\text{polymer}}$ (elastic modulus of silicon tip is 160 GPa versus 0.01–5 GPa for polymers). Then, with a good accuracy, we assume Poisson's ratio $\nu = 0.5$ for all elastomers, $\nu = 0.38$ for PVC, and $\nu = 0.33$ for PS.²¹

After manipulation with initial Sneddon's equations^{12,13} for this model we receive

pyramidal indenter shape

$$E_i = \frac{\sqrt{\pi}}{2\sqrt{2}\beta t g \alpha} (1 - \nu^2) k_n \frac{\Delta z_{\text{defl}, i, i-1}}{h \Delta h_{i, i-1}} \quad (2a)$$

parabolic indenter shape

$$E_i = \frac{1}{2\sqrt{R}\beta} (1 - \nu^2) k_n \frac{\Delta z_{\text{defl}, i, i-1}}{\sqrt{h} \Delta h_{i, i-1}} \quad (2b)$$

where $\beta = A_{\text{cross}}/A$, A_{cross} is the cross-sectional indenter area at the indentation depth h from the apex, β is equal to 2 for elastic deformation of a sphere and $(\pi/2)^2$ for pyramidal and conic shapes,²² α is half of the pyramidal angle of the indenter (we took $\alpha = 35^\circ$ for a typical SFM pyramidal tip), R is the tip radius, and $i, i-1$ refers to the adjacent indenter (tip) displacements.

(18) Bliznyuk, V. N.; Hazel, J. H.; Wu, J.; Tsukruk, V. V. In *Scanning Probe Microscopy of Polymers*; Ratner, B., Tsukruk, V. V., Eds.; 1998; vol. 694, p 252.

(19) Sviridenok, A. I.; Chizhik, S. A.; Petrokovets, M. I. *Mechanics of A Discrete Friction Contact*; Nauka i Tekhnika: Minsk, 1990.

(20) Johnson, K. L.; Kendall, K.; Roberts, A. D. *Proc. R. Soc., London* 1971, A324, 301.

(21) *Polymer Handbook*, Brandrup, J., Immergut, E. H., Eds.; Wiley & Sons: New York, 1975.

(22) Stierman, I. Ya. *Contact Problems in Elastic Theory*; Gostex-izdat: Leningrad, 1952.

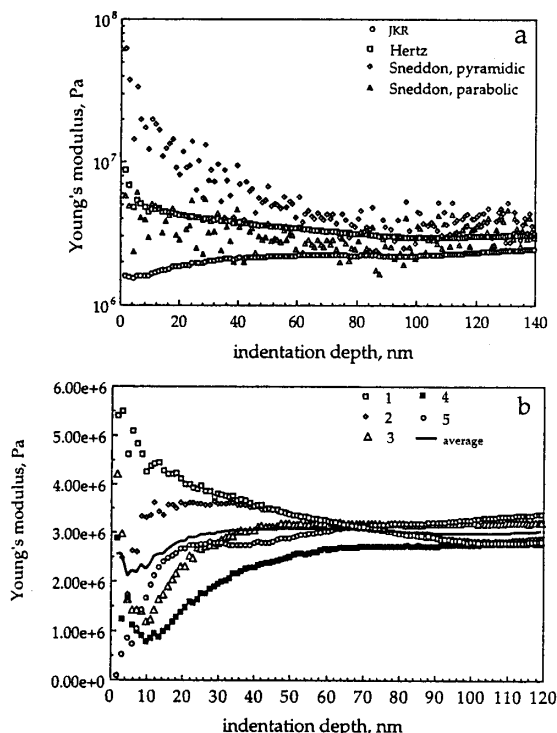


Figure 3. Comparison of different models for evaluation of elastic modulus (a) and modulus versus depth behavior at five different locations for the rubber sample in comparison with the average profile (b).

Derivation of Young's modulus from the Hertzian model gives

$$E_i = \frac{3}{4} (1 - \nu^2) \frac{k_n z_{\text{defl}}}{R^{1/2} h^{3/2}} \quad (3)$$

with the JKR model giving

$$E_i = \frac{9}{4} (1 - \nu^2) R k_n \Delta \left[\frac{P_1}{3Rh} \right]^{3/2} \quad (4)$$

where $P_1 = (3P_2 - 1)[1/9(P_2 + 1)]^{1/3}$, $P_2 = (z_{\text{defl}}/\Delta + 1)^{1/2}$, and Δ is the cantilever deflection at the point where the tip loses contact with the surface.^{19,20}

We used all Sneddon's, Hertzian, and JKR approaches to process the force–distance data and calculate Young's modulus at different penetration depths for rubber material (Figure 3a). As is clear from these data, Young's modulus for elastomeric materials is relatively independent of indentation depth and is virtually constant within 30% at indentation depths larger than 30 nm. Below 30 nm depth, unstable results are obtained which are related to the destabilizing attractive force gradient in the vicinity of surfaces.¹¹ By the repetition of force–distance measurements at different locations we tested the reproducibility of local measurements for polymeric materials studied here. As shown in Figure 3b for the rubber sample, the absolute values of Young's modulus and its indentation depth variation are similar at different locations and give a standard deviation of about 20% (for other materials average standard deviation is about 30%).

All three approaches give convergent results and very close absolute values of Young's modulus at higher

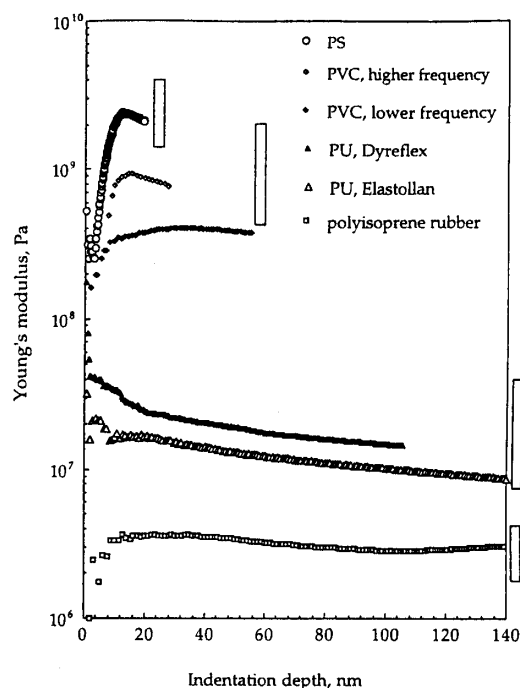


Figure 4. Summarized data for depth variation of the elastic modulus for rubber, two different PUs, PVC at high and low frequencies, and PS. Bars demonstrate the range of elastic bulk modulus variation for a specific material (frequency, molecular weight, and composition dependent).

indentation depths. The absolute value of the rubber Young's modulus is 2.9 ± 0.6 and 2.4 ± 0.5 MPa, as determined by the Hertzian model and JKR models, respectively. Both values are very close to each other and are within the typical range of elastic bulk modulus for polyisoprenes (1–3 MPa).¹⁵ For further calculations, we selected the Hertzian model, which is relatively simple, gives reliable results, and does not require additional speculations or measurements of interfacial energies needed to be known in the JKR theory. At this stage, we have to keep in mind the possibility of up to 20% overestimation of absolute values of Young's modulus calculated with the Hertzian model as compared to the more complete JKR theory.

The Hertzian model was used to calculate depth dependencies of elastic moduli for a set of polymeric materials (Figure 4). The experimental data are shown along with the bars representing the range of Young's modulus measured for bulk materials. Data are presented here at 0.5-Hz frequency of contact. Additional measurements at various frequencies showed very strong frequency dependence for various polymeric materials, as will be discussed in a separate publication.²³ As an example, we demonstrate two very different elastic modulus curves for PVC obtained at high (90 Hz) and low (4.6 Hz) frequencies (Figure 4).

The most important feature of the summary plot in Figure 4 is the very close correlation between the level of elastic moduli probed by SFM and the mechanical properties of bulk materials. For four different types of materials bulk elastic moduli differ by 4 orders of magnitude ranging from 1 to 3 MPa for rubber to 2–5

(23) Tsukruk, V. V.; Huang, Z.; Chizhik, S. A.; Gorbunov, V. V. *J. Mater. Sci.*, submitted.

GPa for PS. SFM data show four distinctive ranges of elastic response at indentation depths in the range 20–200 nm. The absolute value of elastic modulus determined from SFM data *closely correlates with the known bulk moduli for all materials* studied here. The maximum indentation depth for purely elastic deformation varies reciprocally to the elastic properties of materials and depends also upon cantilever stiffness and tip radius. An increase of Young's modulus from 3 MPa for rubber to 50–100 MPa for PUs reduces h_{\max} from 300 to 150 nm, and a further modulus increase to 6 GPa for PS reduces h_{\max} to 20–30 nm.

Conclusions

By combining optimal cantilever parameters and experimental conditions, we can obtain reliable force–distance data which are appropriate for further contact mechanics analysis for a wide selection of polymeric materials. Both Sneddon's and Hertzian models of elastic contact in their complete forms give consistent and reliable results in the range of indentation depths up to 200 nm and correct absolute values of elastic moduli (within 20% deviation) at given experimental conditions which eliminate strong capillary forces.

Calculated elastic moduli of amorphous polymeric materials with homogeneous microstructure are fairly

constant (within $\pm 30\%$) over the entire range of the indentation depths probed up to 200 nm for rubbers and PUs and up to 20–60 nm for PS and PVC. *Close correlation* is observed between elastic moduli determined by SFM and known values for bulk materials. A wide range of elastic polymer properties can be probed if a selection of cantilever stiffness from 0.1 to 50 N/m is available. Elastic moduli can be measured as low as 1 MPa for rubbers to as high as several GPa for glassy polymers with a lateral resolution better 100 nm.

It is also worth noting that some features of elastic deformation such as dynamic behavior vary for different materials studied here and can be discussed in conjunction with their microstructural properties. These and other aspects (such as employment of the more complicated JKR model) will be a subject of a separate publication.²³

Acknowledgment. This work and international collaboration are supported by The National Science Foundation, The Surface Engineering and Tribology Program, CMS-9409431 and CMS-9610408 Grants, and Becton Dickinson Co. Donation of polyurethane materials by BASF and Bayer is highly appreciated. The authors thank J. Hazel for helpful discussion.

LA980042P